Hindawi Publishing Corporation
ISRN Nanomaterials
Volume 2014, Article ID 980206, 6 pages
http://dx.doi.org/10.1155/2014/980206

Research Article

Effect of Growth Temperature on Structural Quality of In-Rich $In_xAl_{1-x}N$ Alloys on Si (111) Substrate by RF-MOMBE

Wei-Chun Chen,[1] Yue-Han Wu,[2] Jr.-Sheng Tian,[2] Tzu-Chun Yen,[2] Pei-Yin Lin,[2] Jr-Yu Chen,[2] Chien-Nan Hsiao,[1] and Li Chang[2]

[1] *Instrument Technology Research Center, National Applied Research Laboratories, 20 R&D Road VI, Hsinchu Science Park, Hsinchu 30076, Taiwan*
[2] *Department of Materials Science and Engineering, National Chiao Tung University, 10010, Tahsueh Road, Hsinchu 30010, Taiwan*

Correspondence should be addressed to Wei-Chun Chen; weichun0809@gmail.com

Received 16 December 2013; Accepted 9 January 2014; Published 23 February 2014

Academic Editors: M. R. Ferreira and B. Panchapakesan

In-rich InAlN films were grown directly on Si (111) substrate by RF-MOMBE without any buffer layer. InAlN films were grown at various substrate temperatures in the range of 460–540°C with TMIn/TMAl ~3.3. Structural properties of InAlN ternary alloys were investigated with X-ray diffraction, scanning electron microscopy, and transmission electron microscopy (TEM). It is shown that the deposited $In_{0.8}AlM_{0.2}N$ (0001) films can be in epitaxy with Si (111) substrate with orientation relationship of $[\bar{2}110]_{InAlN}//[1\bar{1}0]_{Si}$. Also, the growth rate around ~0.25 μm/h almost remains constant for growth in the temperature range from 460 to 520°C. Cross-sectional TEM from InAlN grown on Si (111) at 460°C shows that the epitaxial film is in direct contact with Si without any interlayer.

1. Introduction

The technological importance of group III nitrides GaN, InN, and AlN, particularly for the light-emitting and laser diodes operating in green and blue spectral regions, has stimulated the study of $Al_xGa_{1-x}N$, $In_xGa_{1-x}N$, and $In_xAl_{1-x}N$ alloys. The hexagonal InAlN alloy offers various unique properties which may improve the performance of electronic and optoelectronic devices. InAlN has a direct gap that can be tuned in the range from 6.2 eV for AlN to 0.7 eV for InN [1]. In particular, In-rich InAlN is a promising material for multijunction tandem solar cells [2]. For growth of InAlN in large area at low cost, deposition on Si (111) is of great interest. However, it is difficult to grow In-rich InAlN of single phase, and its epitaxy on Si substrate is also a challenge due to large lattice mismatch. Although reports of InAlN-based devices have been published [3–5], the growth mechanism of InAlN on Si substrate is still unclear.

Previous studies of InAlN growth indicated that the constituent binary components AlN and InN have very different lattice parameters (13.5% mismatch for the a-parameter) and very different optimum growth temperatures (600°C for InN and 1100°C for AlN for metalorganic chemical vapor deposition (MOCVD)). Also, Koide et al. and Zhao et al. indicated the parasitic reaction may prohibit incorporation of Al content and deteriorate the material quality [6, 7]. Particularly, Guo and coworkers [8] fabricated the high quality $Al_xIn_{1-x}N$ films with x being from 0 to 0.14 in the low-Al composition regime using metalorganic vapor phase epitaxy. Due to the difficulties of growth, In-rich $In_xAl_{1-x}N$ layers often exhibit poor crystalline quality. The presence of composition fluctuations and surface hillocks has been reported [9, 10].

Also, silicon is a very promising substrate material for the growth of III-nitride materials. Compared with Al_2O_3, silicon has good thermal conductivity which is especially important for high-power electronic applications [11] and light emitting diodes (LEDs) applications [12]. Various methods have been used to fabricate InAlN films, such as radio-frequency plasma-assisted molecular-beam epitaxy [13], metalorganic chemical vapor deposition [14], pulsed laser deposition [15], and magnetron sputtering [16].

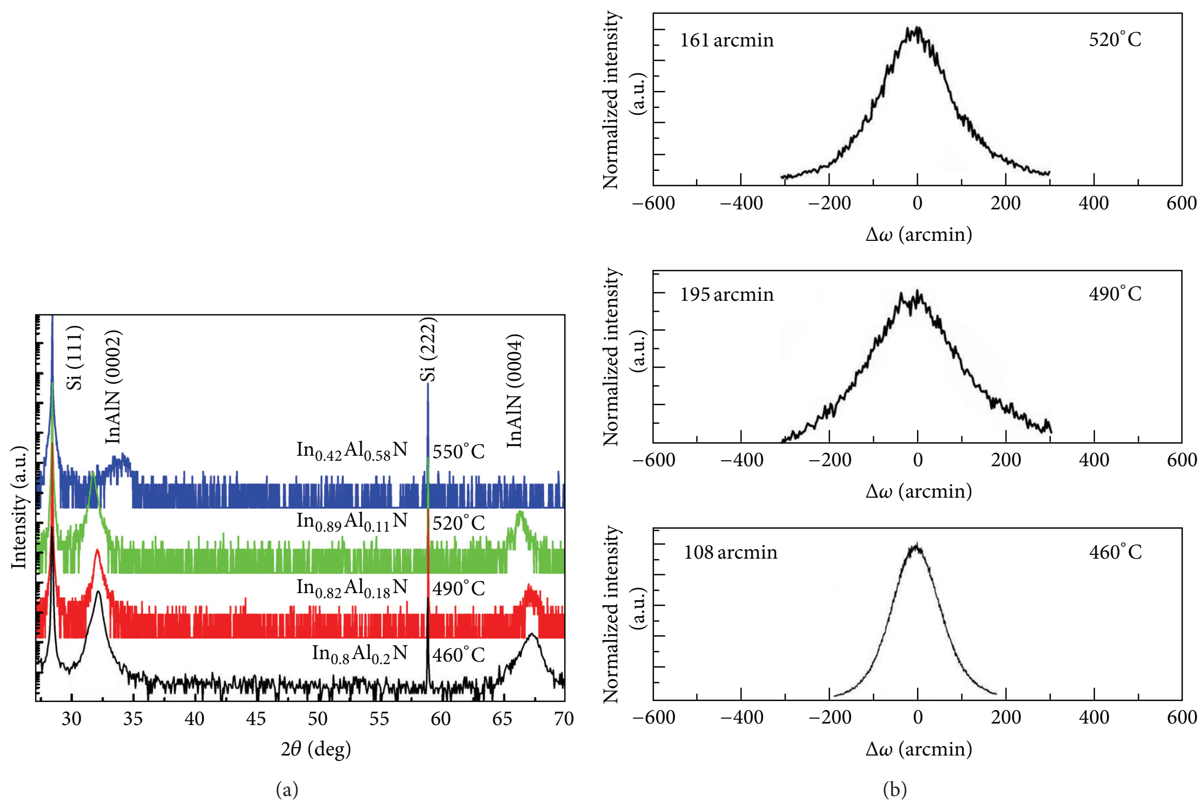

Figure 1: (a) θ–2θ XRD patterns of InAlN films deposited on Si (111) at different temperatures showing varied indium compositions. (b) ω-scan XRD profile of (0002) InN at 460 to 520°C.

However, few studies reported In-rich InAlN thin films growth on Si substrate using radio-frequency metal-organic molecular-beam epitaxy (RF-MOMBE). Compared with the MOCVD growth method, the RF-MOMBE technique generally has the advantage of a low growth temperature for obtaining epitaxial nitride films [17, 18].

In this work, In-rich InAlN/Si (111) heteroepitaxy by RF-MOMBE is studied. Crystalline and surface morphology are characterized by high-resolution X-ray diffraction (XRD), transmission electron microscopy (TEM), and scanning electron microscopy (SEM).

2. Experimental

In-rich $In_xAl_{1-x}N$ alloys were directly grown on p-type Si (111) substrates by RF-MOMBE at different substrate temperatures. Trimethylindum (TMIn : In $(CH_3)_3$) and trimethylaluminum (TMAl : Al $(CH_3)_3$) were used as In and Al sources without carrier gas. TMIn/TMA molar ratio was fixed to 3.3. Nitrogen source was supplied from a RF plasma source (13.56 MHz) with 400 W and the N_2 flow rate of 1 sccm. Prior to loading in the vacuum chamber, the Si (111) substrates were cleaned in a wet bench using Radio Corporation of America processes. Also, the substrate was further wet-etched in buffered oxide etch for 30 s and then dried with N_2, followed by loading into the growth chamber for InAlN deposition. Prior to InAlN growth, the Si (111) substrate was heated at 900°C for 30 min and base pressure of 8×10^{-9} Torr for thermal cleaning of the surface with oxide removal. The substrate temperature was then decreased to 460, 490, 520, and 550°C for growth of In-rich InAlN films. During the deposition, the substrate temperature was monitored with a thermocouple (in contact with heater backside). In the very early stage of deposition both TMIn and TMAl were simultaneously injected into the growth chamber. Nitrogen partial pressure in the growth chamber was stabilized during the growth of $In_xAl_{1-x}N$ films at approximately 1×10^{-5} Torr.

XRD measurements were carried out in a Bruker D8 system using Cu-Kα radiation. The surface morphologies and cross-sectional the $In_xAl_{1-x}N$ films were analyzed using a FE-SEM (Hitachi S-4300) microscope. The detailed microstructure of the InAlN films with interface was investigated by using transmission electron microscopy (TEM) in cross section (Philips Tecnai 20). High-angle annular dark field (HAADF) images were obtained from a JEOL 2010F microscope in scanning transmission electron microscopy (STEM) mode.

3. Results and Discussion

Figure 1 plots θ–2θ XRD patterns for InAlN films grown on Si (111) at various substrate temperatures. The Si (111), Si (222), InAlN (0002), and InAlN (0004) reflections are observed in the patterns, suggesting that the InAlN films may consist of single phase of wurtzite structure. Also, it is seen that the InAlN (0002) peak appears at lower 2θ angle with increasing

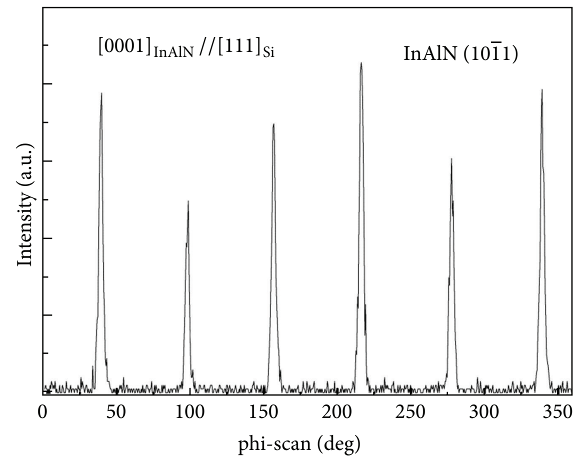

FIGURE 2: (10$\bar{1}$1) phi-scan of $In_{0.8}Al_{0.2}N$ films for 460°C growth.

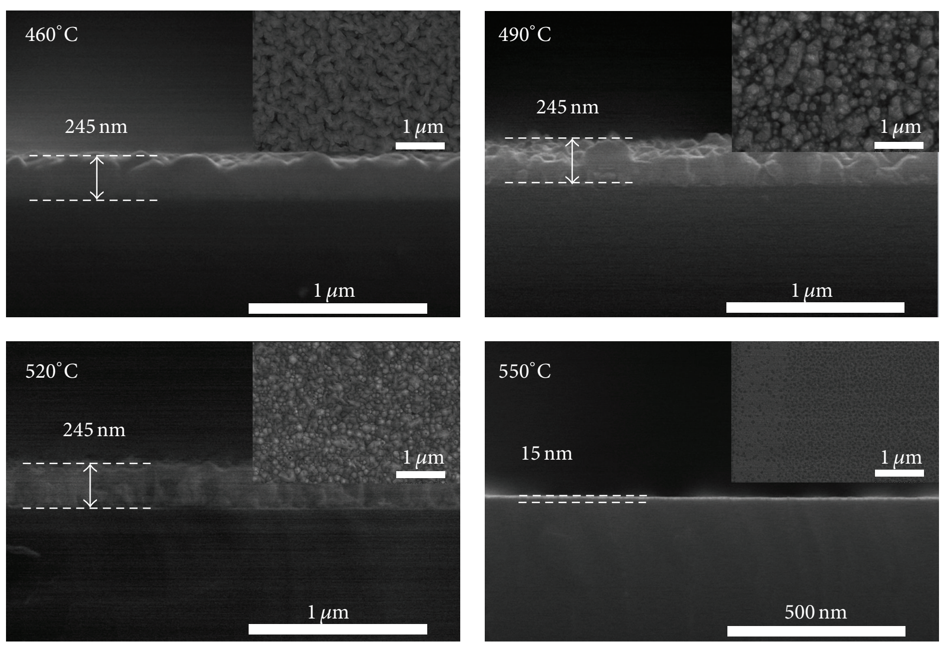

FIGURE 3: Cross-sectional SEM images of $In_xAl_{1-x}N$ films grown on Si (111) with different In compositions. The inset shows surface morphology.

the substrate temperature from 460 to 520°C, whereas it shifts to higher angle for 540°C. Vegard's law has been applied to determine the average In composition of the ternary alloy films via measurement of lattice parameters from HRXRD [19]. The In composition in the deposited $In_xAl_{1-x}N$ films is accordingly determined to be $x = 0.80$ for 460°C, $x = 0.82$ for 490°C, $x = 0.89$ for 520°C, and $x = 0.42$ for 550°C. Also only the (0002)/(0004) peaks are observed without any other reflections for all $In_xAl_{1-x}N$ films, indicating that these films are preferentially grown along the c-axis direction. The reason for In increase with growth temperature from 460 to 520°C might be due to enhanced reaction of TMIn with nitrogen, while Al incorporation into the films is not significantly different at such low temperature from the point of view of AlN formation. However, when the growth of temperature is raised above 520°C, the InN may start to decompose because of its low thermal stability. For growth at 550°C which was close to decomposition temperature of InN [20], lower indium composition was then obtained. For growth above 550°C, InAlN exhibits an extremely weak and broad (0002) peak, suggesting that the crystallinity is poor.

Figure 1(b) shows (0002) X-ray rocking curves (XRC) for InAlN films from which the full-width at half maximum (FWHM) is about 108 arcmin for 460°C, 195 arcmin for 490°C, and 161 arcmin for 520°C, respectively. The higher residual stress in all samples, grown at higher temperature, should be relaxed accomplished with higher defect densities as compared with the InAlN growth at 490°C.

The phi-scan for InAlN (10$\bar{1}$1) reflections from the film grown at 460°C is presented in Figure 2. The diffraction

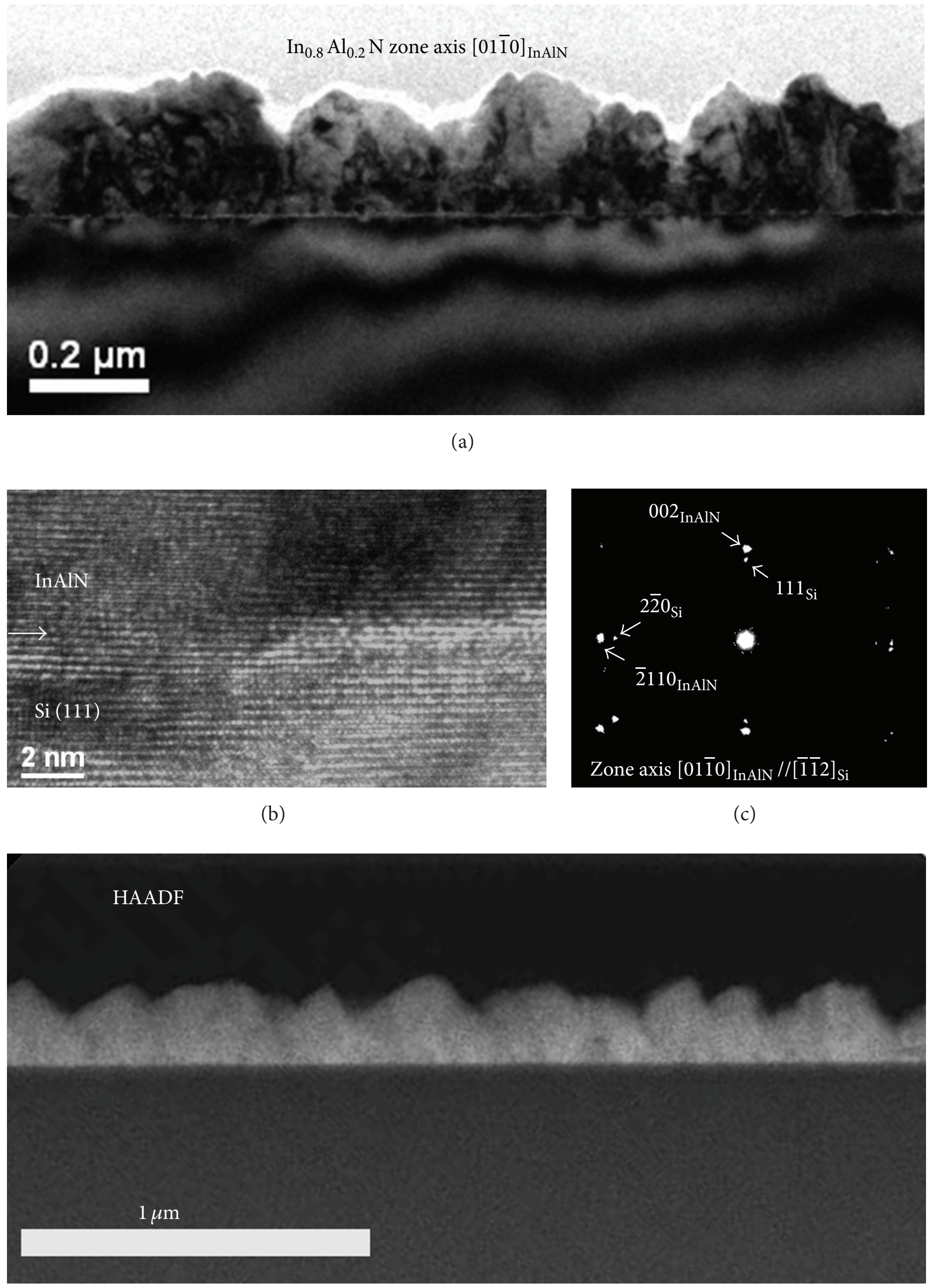

(a)

(b) (c)

(d)

FIGURE 4: (a) Cross-sectional bright field TEM image, (b) the corresponding SAD pattern, (c) HRTEM image, and (d) STEM-HAADF image from $In_{0.8}Al_{0.2}N$/Si (111).

peaks from the $\{10\bar{1}1\}$ plane of InAlN are observed at 60° interval, suggesting that the InAlN film is in epitaxy with Si and part epitaxy with Si. The epitaxial relationship can be deduced from the pattern as $(0002)_{InAlN}//(111)_{Si}$ and $[\bar{2}110]_{InAlN}//[1\bar{1}0]_{Si}$. Similar results were obtained for 490°C and 520°C.

Figure 3 shows top-view and cross-sectional SEM images of the InAlN films grown on Si (111). As estimated from cross-sectional SEM images, the averaged thickness of all the InAlN films grown in the range of 460–520°C is 250 nm from which ~0.25 μm/h is for the growth rate. Though the growth rate is almost unchanged for growth at temperature in the range of 460–520°C, the film thickness of InAlN grown at 550°C is shown to be ~15 nm, which gives a much lower growth rate probably due to low adsorption and high evaporation of In-related species at temperature ≥550°C [21]. The SEM images also reveal that the surface morphology is rough for the substrate temperature ≤520°C. The surface morphology in the insets of top-view images shows 3D grain feature, suggesting that the films are grown in island growth mode.

Figure 4 shows a bright field TEM image of $In_{0.8}Al_{0.2}N$ film (460°C growth temperature) taken from the electron beam direction along the $[01\bar{1}0]_{InAlN}$. The surface morphology of the InAlN film exhibits rough shape as SEM observation. No extra phases appear in the Si substrate or at the interface, implying that In and Al have no reaction with Si as GaN on Si. The corresponding selected-area diffraction pattern (SADP) in Figure 4(b) shows that the main diffraction spots are in the $[01\bar{1}0]_{InAlN}$ zone axis pattern which is parallel to $[\bar{1}\,\bar{1}2]_{Si}$ one. From the SADP, one can see that $(0002)_{InAlN}$ diffraction spot is aligned with $(111)_{Si}$ one and $(2\bar{1}\,\bar{1}0)_{InAlN}$ with $(2\bar{2}0)_{Si}$. Thus, (0001)-oriented hexagonal InAlN has epitaxial relationship with the Si (111) substrate which is the same as observed for AlN and GaN on Si (111) [22, 23]. However, some additional InAlN diffraction spots in the SADP have been observed at locations with deviation angle of approximately 8° from the $[2\bar{1}\,\bar{1}0]$, suggesting that some InAlN grains are slightly misoriented. Since a large fraction of the film is in epitaxy with Si, it HRTEM images are easily observed as shown in Figure 4(c). From the HRTEM image, the InAlN/Si interface is smooth without interlayer. Also, from lattice fringes of the HRTEM image with the corresponding Fourier transform pattern, the same epitaxial relationship as shown in SADP can be obtained. Further verification for the interface can be obtained from the STEM-HAADF image in Figure 4(d) which shows a sharp interface between the InAlN and Si, illustrating that no reactions occur between them. From the Z contrast in the STEM-HAADF image, the intensity in the InAlN film exhibits no significant variation, implying that the indium concentration may have good uniformity in this sample.

4. Conclusions

Direct growth of In-rich InAlN film on Si (111) substrate without any buffer layer by RF-MOMBE has been attempted in the temperature range from 460 to 550°C. All the grown InAlN (0002) films are of single phase and are highly oriented in *c*-axis. The growth rate is almost constant at the substrate temperature in the range of 460–520°C above which it is reduced. HRTEM shows image that epitaxial $In_xAl_{1-x}N$ can be directly grown on Si (111) at about 460°C without any interfacial reactions. The epitaxial relationship is (0001) InAlN//(111) Si with $[\bar{2}110]_{InAlN}//[01\bar{1}0]_{Si}$ and $[01\bar{1}0]_{InAlN}//[\bar{1}\,\bar{1}2]_{Si}$.

Conflict of Interests

The authors declare that there is no conflict of interests regarding the publication of this paper.

References

[1] T. Matsuoka, H. Okamoto, M. Nakao, H. Harima, and E. Kurimoto, "Optical bandgap energy of wurtzite InN," *Applied Physics Letters*, vol. 81, no. 7, pp. 1246–1248, 2002.

[2] R. E. Jones, R. Broesler, K. M. Yu et al., "High efficiency InAlN-based solar cells," in *Proceedings of the 33rd IEEE Photovoltaic Specialists Conference (PVSC '08)*, vol. 1, pp. 1–4, 2008.

[3] S. Senda, H. Jiang, and T. Egawa, "AlInN-based ultraviolet photodiode grown by metal organic chemical vapor deposition," *Applied Physics Letters*, vol. 92, no. 20, Article ID 203507, 2008.

[4] H. Sun, A. R. Alt, H. Benedickter et al., "205-GHz (Al,In)N/GaN HEMTs," *IEEE Electron Device Letters*, vol. 31, no. 9, pp. 957–959, 2010.

[5] C. Ostermaier, G. Pozzovivo, B. Basnar et al., "Metal-related gate sinking due to interfacial oxygen layer in Ir/InAlN high electron mobility transistors," *Applied Physics Letters*, vol. 96, no. 26, Article ID 263515, 2010.

[6] Y. Koide, H. Itoh, N. Sawaki, I. Akasaki, and M. Hashimoto, "Epitaxial growth and properties of $Al_xGa_{1-x}N$ by MOVPE," *Journal of the Electrochemical Society*, vol. 133, no. 9, pp. 1956–1960, 1986.

[7] D. G. Zhao, J. J. Zhu, D. S. Jiang et al., "Parasitic reaction and its effect on the growth rate of AlN by metalorganic chemical vapor deposition," *Journal of Crystal Growth*, vol. 289, no. 1, pp. 72–75, 2006.

[8] Q. X. Guo, N. Itoh, H. Ogawa, and A. Yoshida, "Crystal structure and orientation of $Al_xIn_{1-x}N$ epitaxial layers grown on (0001) \ mbα-Al_2O_3 substrates," *Japanese Journal of Applied Physics*, vol. 34, pp. 4653–4657, 1995.

[9] L. Zhou, D. J. Smith, M. R. McCartney, D. S. Katzer, and D. F. Storm, "Observation of vertical honeycomb structure in InAlNGaN heterostructures due to lateral phase separation," *Applied Physics Letters*, vol. 90, no. 8, Article ID 081917, 2007.

[10] T. C. Sadler, M. J. Kappers, and R. A. Oliver, "The effects of varying metal precursor fluxes on the growth of InAlN by metal organic vapour phase epitaxy," *Journal of Crystal Growth*, vol. 314, no. 1, pp. 13–20, 2011.

[11] J. D. Brown, R. Borges, E. Piner, A. Vescan, S. Singhal, and R. Therrien, "AlGaN/GaN HFETs fabricated on 100-mm GaN on silicon (111) substrates," *Solid-State Electronics*, vol. 46, no. 10, pp. 1535–1539, 2002.

[12] A. Dadgar, C. Hums, A. Diez, F. Schulze, J. Bläsing, and A. Krost, "Epitaxy of GaN LEDs on large substrates: Si or sapphire?" in *Advanced LEDs for Solid State Lighting*, Proceedings of the SPIE, September 2006.

[13] J. Kamimura, T. Kouno, S. Ishizawa, A. Kikuchi, and K. Kishino, "Growth of high-In-content InAlN nanocolumns on Si(111) by RF-plasma-assisted molecular-beam epitaxy," *Journal of Crystal Growth*, vol. 300, no. 1, pp. 160–163, 2007.

[14] T.-T. Kang, M. Yamamoto, M. Tanaka, A. Hashimoto, and A. Yamamoto, "Effect of gas flow on the growth of In-rich AlInN films by metal-organic chemical vapor deposition," *Journal of Applied Physics*, vol. 106, no. 5, Article ID 053525, 2009.

[15] T. Kajima, A. Kobayashi, K. Shimomoto et al., "Layer-by-layer growth of InAlN films on ZnO($000\bar{1}$) substrates at room temperature," *Applied Physics Express*, vol. 3, no. 2, Article ID 021001, 2010.

[16] H. He, Y. Cao, R. Fu et al., "Band gap energy and bowing parameter of In-rich InAlN films grown by magnetron sputtering," *Applied Surface Science*, vol. 256, no. 6, pp. 1812–1816, 2010.

[17] S.-Y. Kuo, F.-I. Lai, W.-C. Chen, and C.-N. Hsiao, "Catalyst-free growth and characterization of gallium nitride nanorods," *Journal of Crystal Growth*, vol. 310, no. 23, pp. 5129–5133, 2008.

[18] S.-Y. Kuo, F.-I. Lai, W.-C. Chen, C.-N. Hsiao, and W.-T. Lin, "Structural and morphological evolution of gallium nitride nanorods grown by chemical beam epitaxy," *Journal of Vacuum Science & Technology A*, vol. 27, no. 4, p. 799, 2009.

[19] H. Angerer, D. Brunner, F. Freudenberg et al., “Determination of the Al mole fraction and the band gap bowing of epitaxial $Al_xGa_{1-x}N$ films,” *Applied Physics Letters*, vol. 71, no. 11, pp. 1504–1506, 1997.

[20] W.-C. Chen, S.-Y. Kuo, F.-I. Lai, W.-T. Lin, C.-N. Hsiao, and D. P. Tsai, “Indium nitride epilayer prepared by UHV-plasma-assisted metalorganic molecule beam epitaxy,” *Journal of Vacuum Science & Technology B*, vol. 29, no. 5, Article ID 051204, 2011.

[21] A. G. Bhuiyan, A. Hashimoto, and A. Yamamoto, “Indium nitride (InN): a review on growth, characterization, and properties,” *Journal of Applied Physics*, vol. 94, no. 5, pp. 2779–2808, 2003.

[22] V. Lebedev, J. Jinschek, U. Kaiser, B. Schröter, W. Richter, and J. Kräußlich, “Epitaxial relationship in the AlN/Si(001) heterosystem,” *Applied Physics Letters*, vol. 76, no. 15, pp. 2029–2031, 2000.

[23] Y. Fu, D. A. Gulino, and R. Higgins, “Residual stress in GaN epilayers grown on silicon substrates,” *Journal of Vacuum Science and Technology A*, vol. 18, no. 3, pp. 965–967, 2000.